PROCEEDINGS OF SPIE

SPIEDigitalLibrary.org/conference-proceedings-of-spie

Towards on-chip spectroscopy based on a single microresonator

Jing Wang, Yuhao Guo, Zhaohong Han, Lionel C. Kimerling, Anu M. Agarwal, et al.

Jing Wang, Yuhao Guo, Zhaohong Han, Lionel C. Kimerling, Anu M. Agarwal, Jurgen Michel, Guifang Li, Lin Zhang, "Towards on-chip spectroscopy based on a single microresonator," Proc. SPIE 10622, 2017 International Conference on Optical Instruments and Technology: Micro/Nano Photonics: Materials and Devices, 1062204 (12 January 2018); doi: 10.1117/12.2296417

SPIE.

Event: International Conference on Optical Instruments and Technology 2017, 2017, Beijing, China

Towards on-chip spectroscopy based on a single microresonator

Jing Wang[1, 2], Yuhao Guo[1, 2], Zhaohong Han[3], Lionel C. Kimerling[3], Anu M. Agarwal[3], Jurgen Michel[3], Guifang Li[1, 2, 4], Lin Zhang[*1,2]

[1]Key Laboratory of Opto-electronic Information Technology of Ministry of Education, School of Precision Instruments and Opto-electronics Engineering, Tianjin University, Tianjin, China

[2]Key Laboratory of Integrated Opto-electronic Technologies and Devices in Tianjin, School of Precision Instruments and Opto-electronics Engineering, Tianjin University, Tianjin, China

[3]Department of Materials Science and Engineering, Massachusetts Institute of Technology, Cambridge, MA 02139, USA

[4]College of Optics and Photonics, CREOL and FPCE, University of Central Florida, Orlando, FL 32816, USA

*Corresponding author: lin_zhang@tju.edu.cn

ABSTRACT

Frequency comb generation in the mid-infrared (mid-IR)region is attractive recently. Here, we propose the Ge-on-Si microresonator for power-efficient frequency comb generation in the mid-IR. An octave-spanning comb can be obtained with power reduced to 190 mW. The robustness of the frequency comb generation with localized spectral loss is also analyzed. Based on the analysis, we propose a novel architecture of on-chip spectroscopy systems in the mid-IR.

Keywords: Integrated optics devices; Nonlinear optics; Microcavities

1. INTRODUCTION

Recently, frequency comb generation in the mid-IR has attracted a lot of attention in spectroscopy and imaging applications [1]. Especially, broadband Kerr frequency combs in mid-infrared are attractive. Some material combinations e.g., chalcogenide glasses and Ge/Si can be used as waveguide core and cladding at >5.5 μm in the deep mid-IR. However, thermal effect becomes more severe, and chalcogenides might suffer from this due to their relatively low thermal conductivity and glass transition temperature. Ge-on-Si waveguides and microresonators would be desirable [2, 3], since Ge has a high refractive index (~4.3), strong nonlinearity, no two-photon and three-photon absorptions beyond 5 μm, and CMOS-compatibility.

Nowadays, several technical challenges for wideband mode-locked Kerr comb generation in the deep mid-IR need to be overcome. Cavity-soliton-based mode-locked combs have their bandwidth related to the following physical parameters:

$$\Delta f_{3dB} \propto \sqrt{\frac{\gamma PF}{|\beta_2|}} \tag{1}$$

where the nonlinear coefficient γ dramatically decreases with wavelength; the cavity finesse F is limited by a high propagation loss in Ge cavities due to sidewall roughness; the pump power P is also limited by narrow-linewidth quantum

2017 International Conference on Optical Instruments and Technology: Micro/Nano Photonics: Materials and Devices, edited by Baojun Li, Xingjun Wang, Ya Sha Yi, Proc. of SPIE Vol. 10622, 1062204 · © 2018 SPIE · CCC code: 0277-786X/18/$18 · doi: 10.1117/12.2296417

cascaded lasers, associated with thermal problem in the mid-IR; and β_2 is the group-velocity dispersion coefficient, which is thus believed to be the key to achieve a wideband mode-locked Kerr frequency comb with a limited pump power. From Eq. 1, we need a flat dispersion curve over a wide band where near-zero dispersion is maintained. However, the previously proposed dispersion flattening technique [4] requires using a low-index material (e.g., SiO_2) to form a slot structure, which is not practical beyond 5 μm because of high material absorption.

On the other hand, across such a wide mid-infrared band, there could often be localized spectral loss mechanisms, including material absorption due to chemical bonds and impurities, mode coupling between polarization states [5], and mode-family crossing of the fundamental mode with a lossy higher-order mode [6]. The effects are deemed detrimental.

Besides, conventionally, for spectroscopy application as shown in Fig. 1(a), a microresonator comb is transmitted through a long waveguide in a gas chamber or a microfluidic channel to increase interaction length and enhance sensing sensitivity. This requires a large chip size. Alternatively, one can fold the long waveguide into a ring cavity in Fig. 1(b) to reduce the area. However, the FSR difference of the two cavities greatly reduces the transmission of the comb. Here, the revealed robustness of mode-locked comb generation with strong localized absorption paves the way to combine the comb generator with the sensing part, in which the nonlinear cavity works as a comb generator and a sensor at the same time. As shown in Fig. 1(c), this would greatly reduce the chip size and guarantee the comb transmission as well. However, this method means that there would be spectral localized absorption peaks, which brings perturbation to comb generation. Up to now, there is little reported on whether mode-locked combs can be successfully generated under such localized spectral molecule absorption perturbation.

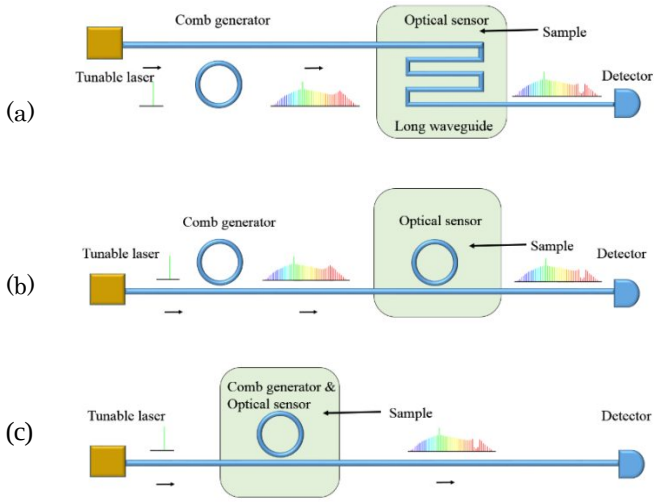

Fig. 1. Three different architectures of comb-based on-chip spectroscopy systems.

Here, our paper is divided in two parts as follows. First, we propose a Ge-on-Si microresonator for power-efficient frequency comb generation in the mid-IR, which is dispersion-flattened without a slot. An octave-spanning Kerr comb can be generated in the deep mid-IR from 2.3 to 8.2 μm (1.8 octaves), which is mode-locked via cavity soliton formation, with the pump power reduced to only 190 mW. Second, we show how to eliminate the impact of strong spectral loss for stable generation of mode-locked Kerr combs with 1 THz wide spectral loss, up to 300 dB/cm. With such robust comb generation, we prove the feasibility of the proposed novel architecture of on-chip spectroscopy systems in mid-infrared region.

2. MID-INFRARED COMB GENERATION

2.1 Resonator configuration

Figure 2 shows the structure of the designed ring cavity for comb generation. Ge waveguide is on the silicon-on-insulator (SOI) platform, and the buried SiO_2 layer is partially etched to avoid strong material absorption beyond 3.8 μm [3], leaving a Si slab to support the Ge waveguide. Structural parameters are: width = 880 nm, Ge height = 2000 nm, Si ridge height = 600 nm, Si slab height = 545 nm and sidewall angle is 87 °.

For our dispersion flattening method, we control optical mode extension from Ge to Si as wavelength increases, which determines the effective refractive index as a function of wavelength. In this work, Ge has a very high index contrast with

air, which causes strong waveguide dispersion. Thus, we change the low-index part (i.e., Si part) from a strip to a ridge/slab structure in Fig. 2 to add one more design freedom in dispersion engineering, while the slab also serves to support the whole waveguide. In principle, the role of the Si part is to allow the mode to extend to Si instead of air so that one can tailor the Si ridge dimensions to control the mode extension and the effective index. We use the fundamental quasi-TM mode. A full-vectorial finite-element method is employed for mode analysis. All material dispersions are taken into account using the Sellmeier equations [3]. As shown in Fig. 3(a), and an ultra-low and flat dispersion is obtained from 4 to 10 μm. γ is calculated over wavelength with the nonlinear index n_2 in [3], which decreases quickly in Fig. 3(a).

Besides, we choose a quite small waveguide width here instead of reducing the waveguide height to suppress the higher-order modes. In this way, we can reduce the number of the higher-order modes without increasing substrate leakage much. Figure 3(b) presents the mode characteristics of this waveguide. There are three higher-order modes at the TM polarization that are adjacent to the fundamental TM mode, i.e., TM_{01}, TM_{02} and TM_{03} modes, respectively. The effective indices of the three modes change with wavelength at different rates, and their cut-off wavelengths are all below the central wavelength (6.6 μm) of the flat-dispersion band in Fig. 3(a).

For the loss considered in our simulation, we assume the scattering loss to be 3 dB/cm. Next, to form a Ge ring resonator based on the proposed waveguide for comb generation, we have to balance between a small mode volume and a high bending loss. We finally choose the bending radius to be 12 um.

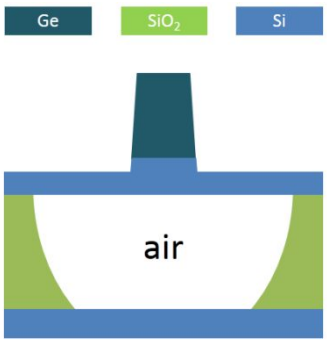

Fig. 2. Cross section of the CMOS-compatible dispersion-flattened Ge-on-Si waveguide with SiO_2 substrate partially removed.

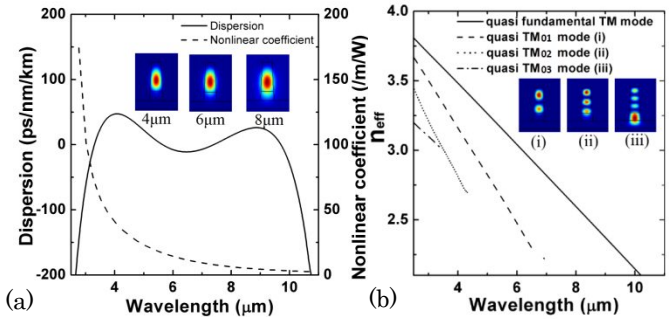

Fig. 3. (a) An ultra-low and flat dispersion (solid) and the nonlinear coefficient (dashed) over a wide wavelength range in the mid-IR. Insets: Mode distribution of the fundamental quasi-TM mode at 4, 6, and 8 μm wavelengths. (b) The effective indices of higher-order TM modes vs. wavelength. The cut-off wavelengths of these higher-order TM modes are shorter than the central wavelength of the low-dispersion band in (a).

2.2 Mid-infrared comb generation

The Q-factor is 40000 at 4.51 μm wavelength with the loss considered above. Our strategy is to have a small effective mode volume to enhance nonlinearity and reduce pump power, while sacrificing the cavity Q-factor a little bit. The free spectral range (FSR) is 1 THz. We then use the Lugiato-Lefever equation to simulate the comb generation with a temporal step of 1 fs. We pump the microresonator at the resonance adjacent to 4.51 μm, and the pump power is 190 mW, which is available from the state-of-the-art quantum cascaded lasers. The comb generation process is seen in Fig. 4, shown by the spectral and temporal snapshots at the normalized pump detuning $\Delta = 0$, 4 and 14.5 (Δ is defined as $2\delta_0/(\alpha+\kappa)$), κ here is 5.188 $\times 10^{-3}$. The comb spectrum becomes increasingly smooth, and accordingly the intra-cavity field evolves into

a pulsed waveform, as a result of a transition of the generated comb from the modulational instability regime to the cavity soliton regime [7], presented by Fig. 4(b). Finally, a single soliton is formed with a full width at half maximum of 17.6 fs and a peak power of 84 W, corresponding to an octave-spanning mode-locked frequency comb from 2.3 to 8.2 μm at -30 dB level. The generated comb has a nonlinear conversion efficiency of 5.13% [8]. In order to understand the pulse characteristic more, we investigate the pulse waveform (solid curve) and frequency chirp (dashed curve) in the time domain in Fig. 5. The soliton is slightly chirped at the pulse peak, and the chirp is around 1.62×10^{-4} rad/fs^2, which can be caused by the unusual dispersion profile mentioned above.

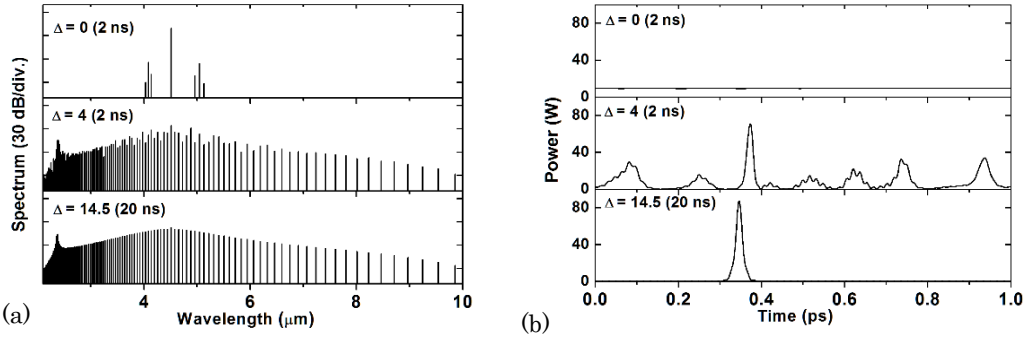

Fig. 4. The comb generation in (a) frequency and (b) time domains at the normalized pump detuning Δ = 0, 4, and 14.5. A Kerr frequency comb is generated by a 190-mW CW pump at 4.51 μm, and the comb is mode-locked via soliton formation.

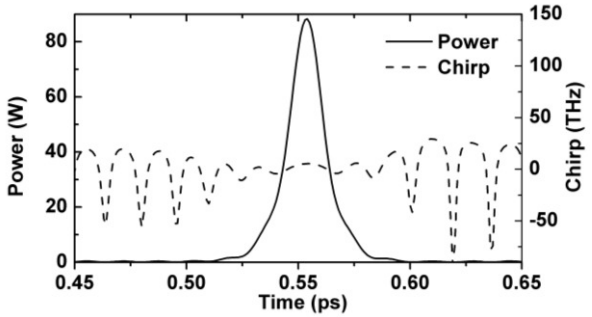

Fig. 5. Pulse waveform (solid curve) and its frequency chirp (dashed curve) in the time domain. The main pulse is slightly chirped.

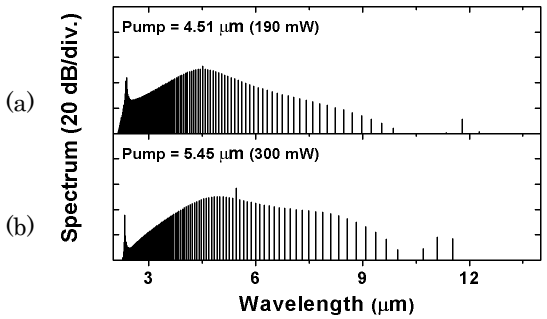

Fig. 6. Pump wavelength is shifted from 4.51 to 5.45 μm, respectively. When the pump is at a long wavelength, the pump power has to be increased due to a small nonlinear coefficient.

The dispersion profile in Fig. 3(a) has a low-dispersion band from 4 to 10 μm wavelength, which gives an advantage for us to widely choose the pump wavelength in this regime. We increase the pump wavelength from 4.51 to 5.45 μm where three-photon absorption is negligible or in absence. For comparison, we keep the X = 14.5, indicating the same normalized pump power. Figure 6(a) shows the generated comb spectra, and we see that the comb can be mode-locked when pumping at 4.51 and 5.45 μm, showing good wavelength feasibility. However, there is no mode-locked comb

obtained at even longer pump wavelengths, due to a smaller nonlinear coefficient in Fig. 3(a) and the increased optical losses. Note that, when pumping at 4.51 μm, only 190 mW pump power is required for the octave-spanning Kerr comb generation, as the nonlinear coefficient is large enough for spectral broadening. In contrast, one needs a pump power of 300 mW, when pumping at 5.45 μm, and the comb bandwidth is from 2.75 to 9.36 μm, as shown in Fig. 6(b).

3. ROBUSTNESS OF COMB GENERATION

As mentioned above, there could be often spectral localized loss mechanism in comb generation. Such loss may be detrimental for Kerr comb generation, especially for octave-spanning comb. In the following part, we study the influence of strong and localized spectral losses on otherwise broadband mode-locked Kerr combs. Note that we consider a Si_3N_4 microresonator in the near infrared region as an example, we believe the principles are still feasible for Ge-Si resonator in the mid-infrared region.

3.1 Modeling

In Fig. 7, the resonator has a FSR of 200 GHz, and the ring waveguide is 1680×730 nm^2, which is on a 3-μm SiO_2 substrate and coated by SiO_2. A bus waveguide is used to couple a pump into the cavity. Propagation loss is 0.2 dB/cm, and the coupling coefficient is 0.0037, corresponding to the cavity Q-factor of 6×10^5. The dispersion property is shown in Fig. 8(a), and we use a pump power of 700 mW at 1420 nm, where the dispersion is -0.014 ps^2/m, and the nonlinear coefficient is 0.96 /m/W. The parameters used here are typical and can be easily achieved in Si_3N_4 microresonators in practice [9, 10].

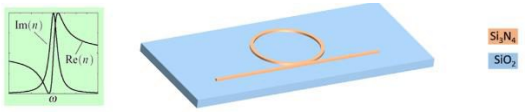

Fig. 7. A Si_3N_4 cavity used for comb generation. The effective index's real and imaginary parts are governed by the Kramers-Kronig relations.

Lugiato-Lefever equation is used for our simulation as follows:

$$\left[\tau_0\frac{\partial}{\partial\tau}+\frac{\alpha}{2}+\frac{\kappa}{2}-j\delta_0+jl\sum_{m=2}^{\infty}\frac{(-j)^m\beta_m}{m!}\frac{\partial^m}{\partial t^m}\right]A(\tau,t)=\sqrt{\kappa}A_{in}-j\gamma l|A(\tau,t)|^2A(\tau,t) \quad (2)$$

where $A=A(\tau,t)$ and A_{in} are intra-cavity field and input pump field (pump power $P_{in}=|A_{in}|^2$). τ and t are the fast and slow times. τ_0 is the round-trip time, and δ_0 is the cavity phase detuning. α is the power loss per round trip, and κ is the power coupling coefficient. The all-order dispersion is used as in [11]. To add the spectrally localized loss to the device, we introduce a Lorentzian-shaped change in the imaginary part of the refractive index, determined by the specified loss value and bandwidth. According to the Kramers-Kronig relations as shown in Fig. 7, the real part of the effective index has an additional change as well. Note that in the following sections, when we mention "loss", we actually mean the joint effects of both loss and its associated phase change.

3.2 Results and discussion

Primary comb lines are first generated due to phase matching as explained in [7], which are responsible for subsequent formation of sub-combs. Thus, we first investigate the influence of the loss located at one of the nearest primary comb lines, at 1508 nm. Figure 8(a) shows the obtained comb, with a strong loss of 300 dB/cm and its FWHM bandwidth of 200 GHz (i.e., one FSR). We can clearly see a sharp intensity dip indicating suppression of comb lines at 1508 nm in the comb spectrum, while there is a peaking effect close to the dip. Note that the comb can still be mode-locked with such a big perturbation, showing great robustness of the comb generation. As a result, a cavity soliton can be seen in Fig. 8(b). The distortion of the soliton pulse in the time domain is believed to be caused mainly by the interference between two strong dispersive waves.

The bandwidth of the spectral loss effect is investigated, varied with the loss peak value kept at 300 dB/cm, centered at one of the nearest primary comb lines at 1508 nm. Figure 9 shows the final spectra with the loss bandwidths of 200 GHz, 600 GHz and 1 THz, i.e., 1, 3, and 5 FSRs, respectively. When the loss bandwidth is increased to 600 GHz, Kerr comb generation is significantly disturbed, stopped at the modulational instability stage with no mode-locked solitons formed anymore. Furthermore, when the loss bandwidth is increased to 1 THz, no comb lines can be generated on the

both sides of the pump, indicating that Kerr comb generation is completely stopped. From above, we see that the localized loss centered at the nearest primary comb lines with a wide bandwidth can be very detrimental to Kerr comb generation. Note that here the localized loss is only added to one side of the pump, which would be the similar to the case with the loss added on the both sides, according to the symmetry of the FWM process.

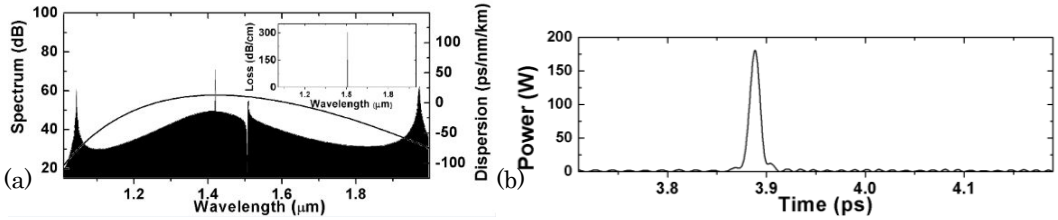

Fig. 8. A spectral loss as large as 300 dB/cm with a FWHM of 200 GHz is added to the primary comb lines closest to the pump. A mode-locked Kerr comb can be generated in (a), associated with a cavity soliton in (b). The inset in (a) shows the attenuation profile of loss peak of 300 dB/cm. The ripples on pulse pedestal are caused by beating between dispersive waves.

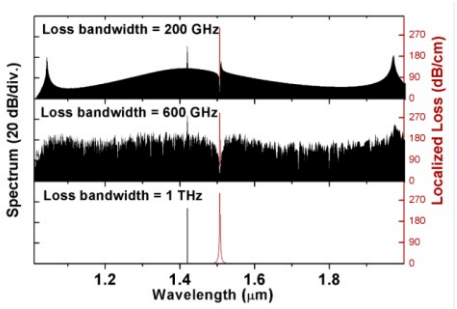

Fig. 9. Different comb generation processes are seen, as the loss bandwidth increases, with the loss of 300 dB/cm at the nearest primary comb lines. The corresponding loss profiles are shown in red lines. The comb is not mode-locked anymore for a loss bandwidth of 600 GHz, while comb generation is completely stopped for a loss bandwidth of 1 THz.

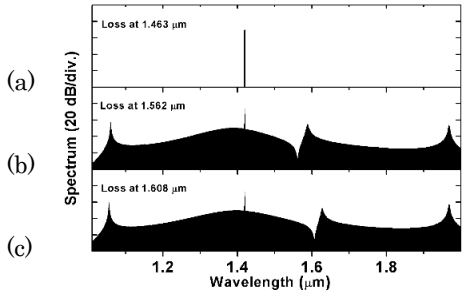

Fig. 10. Mode-locked Kerr combs are obtained as 1-THz-wide loss of 300 dB/cm moves away from the pump, beyond the nearest primary comb lines. This holds even if the loss is at the 2nd nearest primary comb lines.

Next, we examine comb generation by shifting the loss's peak wavelength away from the nearest primary comb lines with a step of 1 THz, when the loss is 300 dB/cm and has a bandwidth of 1 THz. In Fig. 10, the disturbance induced by the strong spectral loss can completely stop the comb generation until shifting the loss peak to 1562 nm, which is about 7 THz away from the nearest primary comb lines. Despite the obvious dip caused by the localized loss, mode-locking as well as wide bandwidth can be both realized with the loss located at 1562 nm in the formed comb. We also check the influence on the comb generation, when such a loss is added on the 2nd nearest primary comb lines at 1608 nm in Fig. 10(c). Solitons can still be formed with such a perturbation. It implies that the effective way to eliminate the detrimental effect of the spectral loss is to properly choose the pump wavelength to make sure that the nearest primary comb lines are far enough away from the loss. Once it is satisfied, the comb spectrum can extend well beyond the lossy region, still being octave-spanning.

The above analysis shows the great robustness for Kerr comb generation, showing the feasibility of the proposed on-chip spectroscopy systems in the mid-infrared region.

REFERENCE

[1] A. Schliesser, N. Picqué, and T. W. Hänsch, "Mid-infrared frequency combs," Nat. Photonics **6**, 440–449 (2012).
[2] R. Soref, "Mid-infrared photonics in silicon and germanium," Nat. Photonics **4**(8), 495–497 (2010).
[3] L. Zhang, A. M. Agarwal, L. C. Kimerling, and J. Michel, "Nonlinear group IV photonics based on silicon and germanium: from near-infrared to mid-infrared," Nanophotonics **3**, 247-268 (2014).
[4] L. Zhang, Y. Yue, R. G. Beausoleil, and A. E. Willner, "Flattened dispersion in silicon slot waveguides," Opt. Express **18**, 20529-20534 (2010).
[5] S. Ramelow, A. Farsi, S. Clemmen, J. S. Levy, A. R. Johnson, Y. Okawachi, M. R. E. Lamont, M. Lipson, and A. L. Gaeta, "Strong polarization mode coupling in microresonators," Opt. Lett. **39**, 5134-5137 (2014).
[6] T. Herr, V. Brasch, J. D. Jost, I. Mirgorodskiy, G. Lihachev, M. L. Gorodetsky, and T. J. Kippenberg, "Mode spectrum and temporal soliton formation in optical microresonators," Phy. Rev. Lett. **113**, 123901 (2014).
[7] T. Herr, V. Brasch, J. D. Jost, C. Y. Wang, N. M. Kondratiev, M. L. Gorodetsky, and T. J. Kippenberg, "Temporal solitons in optical microresonators," Nat. Photonics **8**(2), 145-152 (2014).
[8] C. Bao, L. Zhang, A. Matsko, Y. Yan, Z. Zhao, G. Xie, A. M. Agarwal, L. C. Kimerling, J. Michel, L. Maleki, and A. E. Willner, "Nonlinear conversion efficiency in Kerr frequency comb generation," Opt. Lett. **39**, 6126-6129 (2014).
[9] X. Xue, Y. Xuan, Y. Liu, P-H Wang, S. Chen, J. Wang, D. E. Leaird, M. Qi, and A. W. Weiner, "Mode-locked dark pulse Kerr combs in normal- dispersion microresonators," Nat. Photonics **9**, 594-600 (2015).
[10] J. S. Levy, A. Gondarenko, M. A. Foster, A. C. Turner-Foster, A. L. Gaeta, and M. Lipson, "CMOS-compatible multiple-wavelength oscillator for on-chip optical interconnects," Nat. Photonics **4**, 37-40 (2010).
[11] L. Zhang, Q. Lin, L. C. Kimerling, and J. Michel, "Self-frequency shift of cavity soliton in Kerr frequency comb," arxiv: 14014. 1137 (2014).